

Editorial Manager(tm) for Meccanica
Manuscript Draft

Manuscript Number: MECC305

Title: DYNAMICS OF THE SHIFT IN RESONANCE FREQUENCIES IN A TRIPLE PENDULUM

Article Type: Original papers

Keywords: Triple pendulum; resonance frequency; frequency shift, friction.

Corresponding Author: Dr. José M Sausedo-Solorio, PhD

Corresponding Author's Institution: Universidad Autónoma del Estado de Hidalgo

First Author: Iván Rivas-Camero, Msc

Order of Authors: Iván Rivas-Camero, Msc; José M Sausedo-Solorio, PhD

Abstract: It is shown the solution of a triple pendulum in two dimensions with a harmonic perturbation using a nonlinear model. It is proposed a general matrix form for the model of pendulum with n-links. An analysis of resonance frequencies as well as dynamical states resulting from the variation of magnitude, frequency, and the friction among links is done. It has been found the pendulum can show periodic, quasi-periodic, and chaotic states. A comparison between results of the nonlinear model and its simplification for small oscillations is done. It is shown the analysis of the shift of resonances using transfer functions and numerical calculations.

DYNAMICS OF THE SHIFT IN RESONANCE FREQUENCIES IN A TRIPLE PENDULUM.

Iván Rivas-Cambero* and José Manuel Sausedo-Solorio**

**División de Ingenierías, Universidad Politécnica de Tulancingo*

775 755 8202

irivas@upt.edu.mx

***Centro de Investigación Avanzada en Ingeniería Industrial. Universidad Autónoma del Estado de Hidalgo*

711 717 2000

sausedo@uaeh.edu.mx

Abstract. It is shown the solution of a triple pendulum in two dimensions with a harmonic perturbation using a nonlinear model. It is proposed a general matrix form for the model of pendulum with n-links. An analysis of resonance frequencies as well as dynamical states resulting from the variation of magnitude, frequency, and the friction among links is done. It has been found the pendulum can show periodic, quasi-periodic, and chaotic states. A comparison between results of the nonlinear model and its simplification for small oscillations is done. It is shown the analysis of the shift of resonances using transfer functions and numerical calculations.

Keywords: *Triple pendulum, resonance frequency, frequency shift, friction.*

1 Introduction

In general and whenever possible, in the starting point of any analysis of a system it is used a linear mathematical model. If the model is represented through differential equations, a further step is to propose a more detailed model, increasing the complexity of its equations and solution by using nonlinear differential equations. Due to nonlinearities in a system, some conditions could generate solutions with coexisting attractors or even chaotic behavior [1].

The interest in the study of pendular systems is continuously increasing based on the very rich dynamical behavior it behaves, and because its mathematical model can be used to analyze very complex systems, even it used as a standard benchmark [2]. Despite the general models for an arbitrary number of links used to control issues of the inverted pendulum as in [3], it is well known the lack of general models ready to apply to an n-link regular pendulum. In [4] is proposed a model using equations of motion of the n-link pendulum fixed at upper extreme but using frictionless elements. In [2] a very complete model of a plane pendulum is developed for an arbitrary number of links taking into account friction and compliance, links with variable length and masses. Instead of using

1
2
3
4 previously derived equations for every single additional pendulum link as in [5-8], we
5 propose a general matrix representation for the n-link pendulum with friction, having the
6 characteristic of being able to separate the first derivatives of the dynamical variables,
7 implying a straightforward form for to be solved with a simulation language or package
8 software. Another kind of analysis tool is used in [9], where a symbolic system is used in a
9 mathematical package environment. In [10], it is used a scalable model of a mechanical
10 system, and the comparison between procedures of dynamic simulation is made as is
11 proposed in this work. An interesting analysis is done in [11], there, authors found chaotic
12 dynamics of a triple pendulum, which is controlled with a permanent rotating magneto,
13 using Poincaré sections and graphs in phase space to analyze periodic and chaotic
14 behaviors. Also, in [12] it is proposed a nonlinear model for the comparison between
15 experimental results and calculations of new proposed nonlinear model in the regime of
16 transient chaos. A study of a forced pendulum with nonlinear torsion through bifurcation
17 diagrams behaving period doubling bifurcations to chaos is shown in [13]. Also, it was
18 studied in [14] an experimental observations of chaos in a perturbed pendulum with
19 damping by means of a torque showing alternating behavior.

20
21
22
23
24
25 It is well known that behaviors in real systems are accompanied by both impact forces and
26 the friction as in [15], where authors model a physical plane triple pendulum with barriers
27 causing impacts and sliding, and investigate stability of an orbit in perturbed dynamical
28 systems applying results to a piston-connecting rod-crank of a monkey-cylinder of
29 combustion engine, in order to analyze the noise generated by impacts between the piston
30 and the cylinder. Several practical applications of multiple links pendulum has been done,
31 such as the study of a triple pendulum used in the analysis of the swing of golf club [16],
32 where it is presented an investigation based on the analysis of movement of a robot
33 simulated for human tasks focused in the parameterization of optimal trajectories along
34 time. There, it is done the decomposition of trajectories to characterize how parameters
35 influence in a predictable and controllable form.

36
37
38
39 Pendular systems had been found application in seismic isolation of vibration [17] where,
40 as in this work, it is studied the modal frequency or response of the transference function.
41 Similarly, [18] presents an analytical an experimental studies of a triple pendulum used as
42 insulator of linear seismic movements with a nonlinear viscosity and mechanisms of
43 dissipation of energy of bilinear hysteresis. Another application is found in [19], where a
44 suspension system is studied through different numerical models from triple pendulum with
45 the aim of filtering the high frequencies of the seismic noise. In the same way, in [20] a
46 triple pendulum is used in the suspension of the optical system designed to diminish the
47 effects of both seismic and thermal noise of the suspended masses of a laser interferometer
48 geographic observatory (LIGO). And finally, an interesting optimization procedure can be
49 found in [5], where the response of a triple pendulum by grouping parameters are tested to
50 select the best approximation for a real system.

51
52
53
54
55 In this work the dynamic behavior of a plane triple pendulum is analyzed, it is proposed a
56 mathematical model with weightless-links from a Lagrange equations scheme. The model
57 is written in matrix form readily scalable to any number of links. Harmonic perturbation is
58 applied to the upper link leaving the remaining links free to oscillate. Every link is
59 subjected to friction. Once obtained the equations for an arbitrary number of links, a
60
61
62
63
64
65

particular case for three links is analyzed and numerically solved. The frequency response respect to the friction parameter is obtained finding a shift in the resonance peaks for every link. To verify the nonlinear model, a simplified version for small oscillations is obtained and compared with other results [12-14] using reduced linear models for the triple pendulum.

The structure of this work is as follows. In section 2 the development of a matrix nonlinear model for a pendulum with an arbitrary number of links is shown, also it is obtained a particular case of a three links system (triple pendulum). In section 3 the separation on a matrix form of the first derivatives of dynamical variables is done in order to use any software tool or programming language to solve it. In section 4, results of the frequency response are shown and compared with analytical calculations using integral transform and obtaining the transference function. In section 5 it is showed the main results of the work namely, the shift of the frequency resonances and its relation to the friction parameter. Finally conclusions are left to section 6.

2. Development of the mathematical model.

The mathematical model for a multi link pendulum can be built based on the Euler-Lagrange formulation [21],

$$\frac{d}{dt} \frac{\partial L}{\partial \dot{\theta}_k} - \frac{\partial L}{\partial \theta_k} + \frac{\partial Q}{\partial \dot{\theta}_k} = 0 \quad (1)$$

where $L = T - u$ is the Lagrangian defined as the difference between kinetic and potential energy, Q are the friction losses and θ_k are the generalized coordinates. For a multi-link pendulum, the components of Lagrangian function are: $T = \frac{1}{2} \sum m_k |r_k \dot{\theta}_k|^2$,

$u = g \sum m_k h_k$ and $Q = \frac{1}{2} \sum R_k (\dot{\theta}_k - \dot{\theta}_{k-1})^2$. After replacing these terms in Eqn. (1), we can establish a non linear differential equations system in a matrix form for a pendulum with an arbitrary number of links as:

$$M_N(\theta) \ddot{\theta}_N + N_N(\theta) \dot{\theta}_N^2 + R_N \dot{\theta}_N + P_N(\theta) + f_N(\theta, t) = 0 \quad (2)$$

Where M_N , N_N , R_N , P_N , and f_N are matrices given by:

$$M_N(\theta) = \begin{bmatrix} M_1 & M_{12} \cos(\theta_1 - \theta_2) & M_{13} \cos(\theta_1 - \theta_3) & \cdots & M_{1n} \cos(\theta_1 - \theta_n) \\ M_{12} \cos(\theta_1 - \theta_2) & M_2 & M_{23} \cos(\theta_2 - \theta_3) & \cdots & M_{2n} \cos(\theta_2 - \theta_n) \\ M_{13} \cos(\theta_1 - \theta_3) & M_{23} \cos(\theta_2 - \theta_3) & M_3 & \cdots & M_{3n} \cos(\theta_3 - \theta_n) \\ \vdots & \vdots & \vdots & \ddots & \vdots \\ M_{1n} \cos(\theta_1 - \theta_n) & M_{2n} \cos(\theta_2 - \theta_n) & M_{3n} \cos(\theta_3 - \theta_n) & \cdots & M_n \end{bmatrix}$$

$$N_N(\theta) = \begin{bmatrix} 0 & M_{12} \sin(\theta_1 - \theta_2) & M_{13} \sin(\theta_1 - \theta_3) & \cdots & M_{1n} \sin(\theta_1 - \theta_n) \\ -M_{12} \sin(\theta_1 - \theta_2) & 0 & M_{23} \sin(\theta_2 - \theta_3) & \cdots & M_{2n} \sin(\theta_2 - \theta_n) \\ -M_{13} \sin(\theta_1 - \theta_3) & -M_{23} \sin(\theta_2 - \theta_3) & 0 & \cdots & M_{3n} \sin(\theta_3 - \theta_n) \\ \vdots & \vdots & \vdots & \ddots & \vdots \\ -M_{1n} \sin(\theta_1 - \theta_n) & -M_{2n} \sin(\theta_2 - \theta_n) & -M_{3n} \sin(\theta_3 - \theta_n) & \cdots & 0 \end{bmatrix}$$

$$R_N = \begin{bmatrix} R_1 + R_2 & -R_2 & 0 & \cdots & 0 \\ -R_2 & R_2 + R_3 & -R_3 & \cdots & 0 \\ 0 & -R_3 & R_3 + R_4 & \cdots & 0 \\ \vdots & \vdots & \vdots & \ddots & \vdots \\ 0 & 0 & 0 & \cdots & R_n \end{bmatrix}$$

$$P_N(\theta) = \begin{bmatrix} A_1 g \sin \theta_1 \\ A_2 g \sin \theta_2 \\ A_3 g \sin \theta_3 \\ \vdots \\ A_n g \sin \theta_n \end{bmatrix}, \quad f_N(\theta, t) = \begin{bmatrix} A_1 \cos \theta_1 \\ A_2 \cos \theta_2 \\ A_3 \cos \theta_3 \\ \vdots \\ A_n \cos \theta_n \end{bmatrix} \eta$$

In this work a two dimensional pendular system containing three link and masses are considered. The schematic representation of this system is shown in figure 1, the masses and links lengths are labeled as m_1, m_2, m_3 and L_1, L_2, L_3 , respectively, and angles θ_1, θ_2 , and θ_3 , between each link and a vertical line. The whole system is subjected to a harmonic disturbance $\eta = \eta_0 \cos \omega t$ applied to of the upper link.

From figure 1, dynamical variables can be written as: $x_1 = L_1 \sin \theta_1, y_1 = -L_1 \cos \theta_1, x_2 = x_1 + L_2 \sin \theta_2, y_2 = y_1 - L_2 \cos \theta_2, x_3 = x_2 + L_3 \sin \theta_3, y_3 = y_2 - L_3 \cos \theta_3$

Using the general model (2) it is forward to write the case for the triple pendulum. The term for losses are given by [21]:

$$Q = \frac{1}{2} R_1 \dot{\theta}_1^2 + \frac{1}{2} R_2 (\dot{\theta}_2 - \dot{\theta}_1)^2 + \frac{1}{2} R_3 (\dot{\theta}_3 - \dot{\theta}_2)^2$$

where R_1, R_2, R_3 , are the friction coefficients corresponding to each joint. Kinetic energy for every mass m_i is $T_i = \frac{1}{2} m_i |\dot{r}_i|^2, i=1, 2, 3$; so, term for total kinetic and potential energy are :

$$T = \frac{1}{2} m_1 |\dot{r}_1|^2 + \frac{1}{2} m_2 |\dot{r}_2|^2 + \frac{1}{2} m_3 |\dot{r}_3|^2 \quad \text{and} \quad u = m_1 g h_1 + m_2 g h_2 + m_3 g h_3;$$

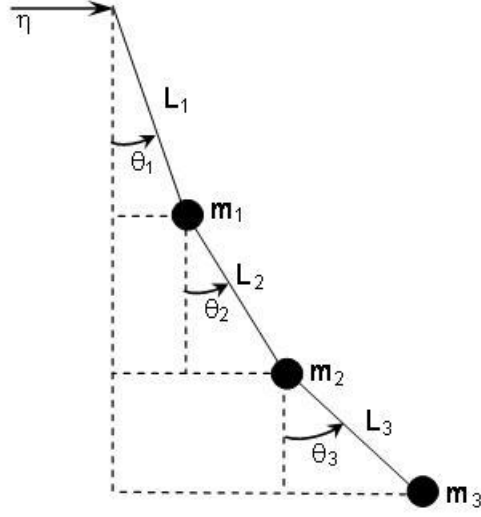


Figure 1 Schematic representation of a triple pendulum with a perturbation in the upper link.

where r_1, r_2, r_3 , and h_1, h_2, h_3 , are length links and vertical distances respectively. Doing substitutions in equation (3), the mathematical model is depicted in a matrix format, as follows:

$$M(\theta)\ddot{\theta} + N(\theta)\dot{\theta}^2 + R\dot{\theta} + P(\theta) + f(\theta, t) = 0 \quad (3)$$

where

$$M(\theta) = \begin{bmatrix} M_1 & M_{12} \cos(\theta_1 - \theta_2) & M_{13} \cos(\theta_1 - \theta_3) \\ M_{12} \cos(\theta_1 - \theta_2) & M_2 & M_{23} \cos(\theta_2 - \theta_3) \\ M_{13} \cos(\theta_1 - \theta_3) & M_{23} \cos(\theta_2 - \theta_3) & M_3 \end{bmatrix}$$

$$N(\theta) = \begin{bmatrix} 0 & M_{12} \sin(\theta_1 - \theta_2) & M_{13} \sin(\theta_1 - \theta_3) \\ -M_{12} \sin(\theta_1 - \theta_2) & 0 & M_{23} \sin(\theta_2 - \theta_3) \\ -M_{13} \sin(\theta_1 - \theta_3) & -M_{23} \sin(\theta_2 - \theta_3) & 0 \end{bmatrix}$$

$$R = \begin{bmatrix} R_1 + R_2 & -R_2 & 0 \\ -R_2 & R_1 + R_2 & -R_3 \\ 0 & -R_3 & R_3 \end{bmatrix} \quad P(\theta) = \begin{bmatrix} A_1 g \sin \theta_1 \\ A_2 g \sin \theta_2 \\ A_3 g \sin \theta_3 \end{bmatrix} \quad f(\theta, t) = \begin{bmatrix} A_1 \cos \theta_1 \\ A_2 \cos \theta_2 \\ A_3 \cos \theta_3 \end{bmatrix} \dot{\eta}$$

and M_k and A_k terms are defined as: $M_1 = (m_1 + m_2 + m_3)L_1^2$, $M_2 = (m_2 + m_3)L_2^2$,
 $M_3 = (m_3)L_3^2$, $M_{12} = (m_2 + m_3)L_1L_2$, $M_{13} = (m_3)L_1L_3$, $M_{23} = (m_3)L_2L_3$, $A_1 = (m_1 + m_2 + m_3)L_1$,
 $A_2 = (m_2 + m_3)L_2$, and $A_3 = (m_3)L_3$.

The well known special case of a linear (small oscillations) triple pendulum published elsewhere can be obtained from Eq. (2). This shown in appendix A.

3. Numerical solutions

In this work, it is proposing a way to solve Eqn. (3) by transforming the second order differential equations system into a first order non linear system stated in matrix from as:

$$d\theta = M_a(\theta)^{-1}[-N_a(\theta)v_a - P_a(\theta) - f_a(\theta, t)] \quad (4)$$

where: $d\theta = [\dot{u} \ \dot{v} \ \dot{w} \ \dot{\theta}_1 \ \dot{\theta}_2 \ \dot{\theta}_3]^T$; $v_a = [u^2 \ v^2 \ w^2 \ -u \ -v \ -w]^T$ are vectors of six dimensions, and

$$M_a(\theta) = \begin{bmatrix} M(\theta) & R \\ 0 & I \end{bmatrix}; \quad N_a(\theta) = \begin{bmatrix} N(\theta) & 0 \\ 0 & I \end{bmatrix}; \quad P_a(\theta) = \begin{bmatrix} P(\theta) \\ 0 \end{bmatrix};$$

$$f_a(\theta, t) = \begin{bmatrix} f(\theta, t) \\ 0 \end{bmatrix}, \quad I = \begin{bmatrix} 1 & 0 & 0 \\ 0 & 1 & 0 \\ 0 & 0 & 1 \end{bmatrix}$$

are 6x6 partitioned matrix Here, u , v , w , θ_1 , θ_2 , and θ_3 are the new variables. Continuing with validation of our main model (Eqn. 3), called from here *full model*, it has been done numerical calculations to compare with the correspondent small oscillations model (Eqn. A-2). In this way, figure 2 shows a typical time series for the angular displacement of third angle. One curve was obtained with the small oscillations model (called from here *short model*); and the other one with the full model. Both curves were obtained for the same set of parameters and initial conditions. For a sake of comparison, the effect of friction is ignored, and values for perturbation frequency and amplitude perturbation are $f=0.5$ Hz and $\eta=0.05$ m, respectively. Masses and lengths have the same values $m_i=1$ kg and $l_i=1$ m respectively.

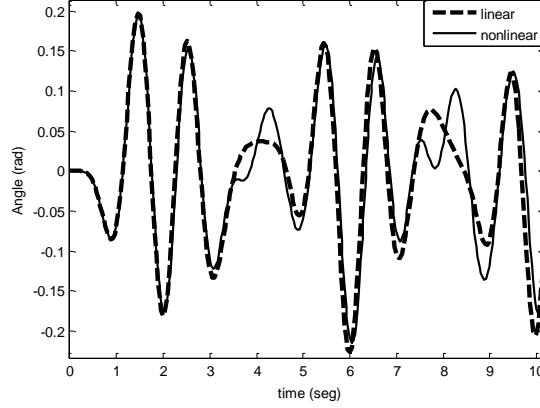


Figure. 2 Comparison between response of the linear model and nonlinear model in time series for the behavior of the third angle, with perturbation frequency $f=1$ Hz. Both curves were obtained with the same parameters and initial conditions.

The non linear pendulum, as it is well known, behaves several states, such as periodic, quasi-periodic and chaotic, characteristic behavior obtained from our non linear model are shown here for completeness in figure 3. In this figure are shown time series curves for θ_3 and phase space curves for θ_1 vs. θ_3 angles. Curves in this figure were obtained by varying the frequency of perturbation and the damping constant equal to 1.0 , 0.1 , and 0.01 Nm/s^2 in every joint.

4 Frequency response analysis.

Another interesting comparison between the two models is obtained by calculating bifurcation diagrams to observe the frequency response. Figures 4 and 5 show the resonance peaks as the perturbation frequency is varying. Although the first peak is the same for both models, for $f > 0.5$ Hz the last two resonance peaks are lost for the full model this is because the non-linearities start to influence in the pendulum behavior.

The other further analysis to verify the correctness for the proposing model, was done by using the transfer function of the system. Using (A-1) in the form $ML\ddot{\theta} + R\dot{\theta} + gml\theta = -ml\ddot{\eta}$.

By applying Laplace transform can be written as: $MLs^2\theta(s) + Rs\theta(s) + gml\theta(s) = -mls^2\eta(s)$

or $(MLs^2 + Rs + gml)\theta(s) = -mls^2\eta(s)$

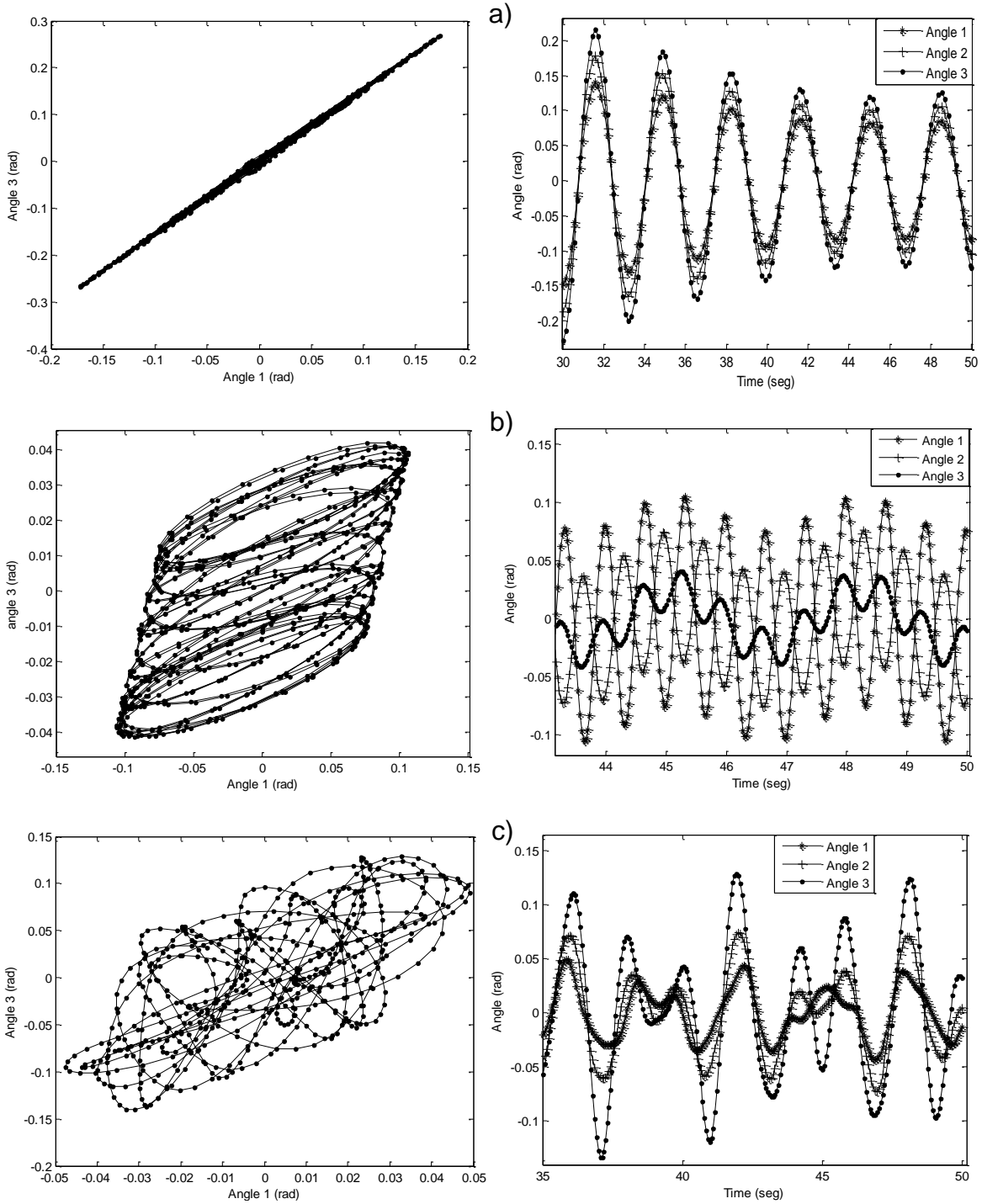


Figure. 3 It is shown different states typical of the pendulum obtained by varying the perturbation frequency and damping. a) Periodic state with $f=0.3$ Hz, damping of 1 Nm/s^2 , b) Cuasi-periodic state with $f=1.5$ Hz, damping of 0.1 Nm/s^2 and c) Chaotic state with $f=0.5$ Hz, damping of 0.1 Nms^2 . Curves for the three angles corresponding to each link are shown in the time series graphs, but curve for the third angle is darker. In phase space are plotting angle θ_1 against θ_3 .

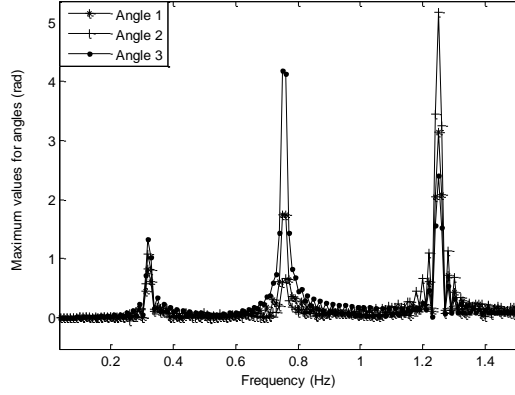


Figure 4, Frequency response for the small oscillations model. It is shown three resonance frequencies for each angle.

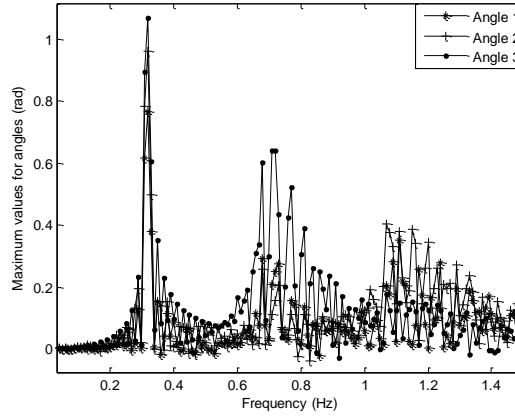


Figure 5, Frequency response for the full nonlinear model. It is shown three resonance frequencies for each angle.

where $\theta(s)$ is the output variable. Transfer function is defined as the rate of output to input variable:

$$\frac{\theta(s)}{\eta(s)} = - \frac{m l s^2}{(M L s^2 + R s + g m l)} \quad (5)$$

Frequency response analysis of the system respect is displayed in figure 6. Numerical analysis is done through Eqn. (5), with $s=j\omega$, and $\omega=2\pi f$ and using same constants as in previous calculations to get figure 4. It can be seen the three resonance frequencies and the same behavior of nonlinear model i.e. the first resonance is clearly defined while the last two are considerably attenuate.

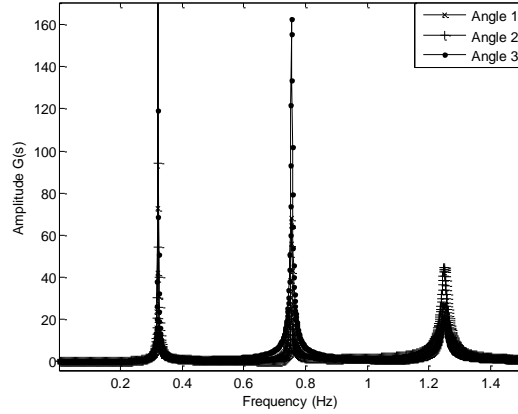


Figure. 6 Frequency response diagram using Laplace transform shows the same behavior as using differential equation solution.

5 Shift in resonance frequency.

It has been done a study of the dynamical properties of the triple pendulum as the damping in the junction varies. First, in analyzing the behavior of the system around the frequency resonances peaks, it has been found, a slowly exponential decaying in the maximum amplitude of angles as friction coefficient increases. This is shown in the figure 7, where vertical axis correspond to the maximum angle reach for every link and horizontal axis to the variation of the friction coefficient keeping the same for all links ranging from 0 to 1 Nm/s^2 . These curves have an exponential decay with a scaling law of approximately 0.50 i.e. $\theta_{max} \sim e^{-0.5R}$. Second, it has found that resonance frequencies behave a shift with changes in the friction. The behavior of this shift for the second resonance frequency peak is shown in figure 8 for the three angles of the system, where, to obtain every curve the range of frequency value was varied in the range 0.63 to 0.75 Hz, and friction constant in the range 0 to 0.5 Nm/s^2 .

Two different behaviors have been found as the friction varies in the joints. A behavior where shift is independent for small values of the friction parameter meaning that for $R_k < 0.1$, the friction does not displace the picks of resonance; the same behavior happens for $R_k > 0.3$. In the middle, for values of R ranging from 0.1 to 0.3, a linear behavior has been obtained meaning that the shift in resonance peaks grows lineally with the friction with a slope of 0.25 i.e. $\Delta f_r = 0.25R$.

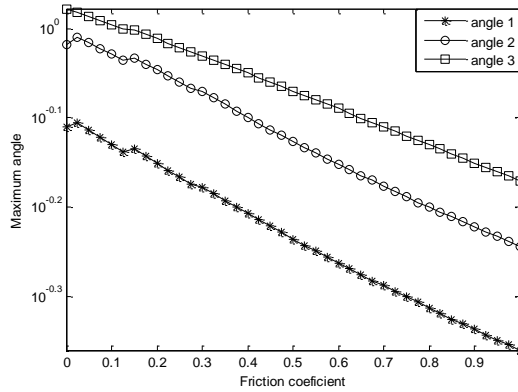


Figure. 7 Maximum values in steady state for each angle using a frequency equal to the first resonance peak.

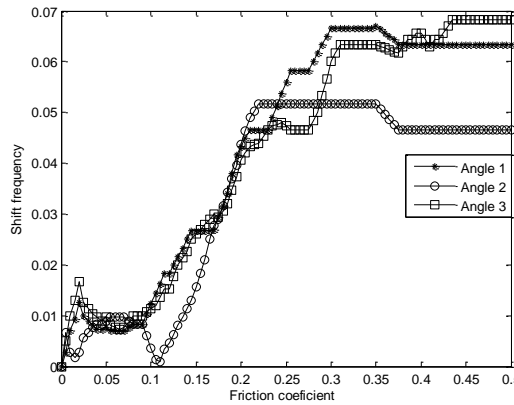


Figure. 8 This is a behavior for the shift of the second resonance frequency peak. Two different behaviors can be seen, one where friction does not influence the peak in frequency and other where the shift grows linearly with damping parameter.

6 Conclusions

For a non linear matrix model based on a Lagrangian formulation obtained for a pendulum with n-links has been proven its applicability and simplicity of use based on the representation stated here (with the first derivatives of the dynamic variables yet separated). Such representation has a direct implementation in a computational language or software package, so it can be written directly a model for a pendulum with any number of links.

Using the special case for three links, a model has been obtained in full agreement with models stated elsewhere for three links. Our non-linear model were validated using a linearized (or small oscillations) version by getting time series graphs with similar dynamic behavior in the limit case.

In the analysis made for the frequency response, three different strategies were used to compare picks of resonance, one by means of the linear model, other by using transfer functions based on Laplace transform, and with our non-linear model. The comparison of the position of the peaks of resonance in each case in almost exact, validating in this way our model.

1
2
3
4 A last main result has been obtained in the analysis of the shift of frequency resonances. It
5 had been observed two distinct behaviors, one where the friction in the joints does not
6 affect such resonances and other where the shift in the frequency of resonance follows a
7 linear scaling law.
8
9

10 Having laws governing the behavior of a system is critical in the design of a structure or
11 mechanism, so this works provides a method for analyzing how the resonance frequency
12 peaks behave in the case of a changing in the parameter of the system.
13
14

15 16 17 **7 References**

- 18 1. Lara Luis, Stoico César, Machado Rodrigo, Castagnino Mario (2003). "Estimación de exponentes de
19 Lyapunov", Mecánica Computacional Vol. XXII, Bahía Blanca, Argentina.
- 20 2. Grossman Martin, Gmitterko Alexander, (2008) *N-link inverted pendulum, LQR control, some*
21 *observations*, AT&P plus1
- 22 3. Lobas, L.G. (2007), "The equations of an inverted pendulum with an arbitrary number of links and an
23 asymmetric follower force", Int. Appl. Mech. Vol. 43, No. 5.
- 24 4. Campbell, S.L., Chancelier, J.P., and Nikoukhah R (2006), "Modeling and Simulation in Scilab/Scicos",
25 Chap. 5, Springer N.Y.
- 26 5. Awrejcewicz Jan and Kudra Grzegorz (2008). "Dynamics of a real triple pendulum – modeling and
27 experimental observation", ENOC 2008, Saint Petersburg, Russia, June 30–July 4.
- 28 6. Awrejcewicz Jan, Kudra Grzegorz, Wasilewsky Grzegorz (2007). "Experimental and numerical
29 investigation of chaotic regions in the physical pendulum", Nonlinear Dynamic, 50:755-766.
- 30 7. Kim, D., Singhose, W.(2006), "Reduction of double-pendulum bridge crane oscillations", 8th Int. Conf. on
31 Motion and Vib. Ctl.
- 32 8. Husman, M. E. , Torrie, C. I. , Plissi, M. V. , Robertson, N. A. , Strain, K. A. and Hough, J. (2000),
33 "Modeling of multistage pendulums: Triple pendulum suspension for GEO 600" Rev. Sci. Instr. Vol. 71,
34 No. 6
- 35 9. Grossman, Martin (2007), *N-link inverted pendulum, general energy equation*, AT&P J. Plus1.
- 36 10. Schmitt, Alfred A., Bender, Jan S. (2005). "Impulse based dynamic simulation of multibody systems:
37 numerical comparison with standard methods", Proc. Automation of Discrete Production Engineering, pp.
38 324-329.
- 39 11. Berdahl John P. and Vander Lugt Karel (2001). "Magnetically driven chaotic pendulum", Am. J. Phys.,
40 Vol. 69, No. 9, pp 1016-1019.
- 41 12. Sousa de Paula Aline, Amorin Savi and Lunes Pereira-Pinto Francisco Heitor (2006). "Chaos and
42 transient in an experimental nonlinear pendulum", Journal of sound and vibration, volume 294, Issue 3,
43 pages 585-595.
- 44 13. Beckert, S., Schock, U. Schulz, C. D., Weidlich, T., Kaiser, F. (1987), "Experiments on the bifurcation
45 behavior of a forced nonlinear pendulum", Phys Lett. A107, 347-350.
- 46 14. Blackburn, J. A., Yang, Z. J., Vik, S. (1987), "Experimental study of chaos in a driven pendulum."
47 Physica D26, 385-395.
- 48 15. Awrejcewicz Jan, Kudra Grzegorz (2007). "The triple pendulum with barriers and the piston-connecting
49 rod-crankshaft model", Journal of theoretical and applied mechanic, 45, 1, pp. 15-23.
- 50 16. Aicardi Michele (2007). "A triple pendulum robotic model and a set of simple parametric functions for the
51 analysis of the golf swing", International Journal of Sport Science and Engineering, Vol. 1 No. 2 pp. 75-
52 86.
- 53 17. Wu, Wan (2007). *Instrumentation of the next generation gravitational wave detector: Triple pendulum*
54 *suspension and electro-optic modulator*, Thesis Diss., University of Florida, USA.
- 55 18. Morgan, Troy A (2007). *The use of innovative base isolation systems to achieve complex seismic*
56 *performance objective*, PhD dissertation, University of California, Berkeley, USA.
- 57 19. Ruet, Laurent (2007). "Active control and sensor noise filtering duality application to advanced LIGO
58 suspension", Thesis, Ins. Nat. Sci. App. de Lyon.
- 59
60
61
62
63
64
65

- 1
2
3
4 20. Plissi M. V., Torrie C. I. and Barton M., Robertson N. A. (2004). "An investigation of eddy-current
5 damping of multi-stage pendulum suspensions for use in interferometric gravitational wave detector",
6 Rev. Sci. Intr., Vol. 75, No. 11.
7 21. Golstein Helbert, Poole Charles Safko John (2003). *Classical Mechanics*, Third edition, Addison Wesley.
8
9

10 Appendix A

11 Obtaining small oscillations model from the non linear model.

12
13
14
15 In order to validate above model of Eqn. (2), the most known linear case of small
16 oscillations can be obtained from it ($\sin \theta \approx \theta$), resulting for a n-link pendular systems with
17 small oscillations. From the linear model with an arbitrary number of links,
18

$$19 M_N L_N \ddot{\theta}_N + R_N \dot{\theta}_N + g m_N l_N \theta_N + m_N l_N \eta_{Na} = 0$$

20 where:

$$21 M_N = \begin{bmatrix} m_1 L_1 & m_2 L_1 & m_3 L_1 & \cdots & m_n L_1 \\ 0 & m_2 L_2 & m_3 L_2 & \cdots & m_n L_2 \\ 0 & 0 & m_3 L_3 & \cdots & m_n L_3 \\ \vdots & \vdots & \vdots & \ddots & \vdots \\ 0 & 0 & 0 & \cdots & m_n L_n \end{bmatrix}; \quad L_N = \begin{bmatrix} L_1 & 0 & 0 & \cdots & 0 \\ L_1 & L_2 & 0 & \cdots & 0 \\ L_1 & L_2 & L_3 & \cdots & 0 \\ \vdots & \vdots & \vdots & \ddots & \vdots \\ L_1 & L_2 & L_3 & \cdots & L_n \end{bmatrix};$$

$$22 R_N = \begin{bmatrix} R_1 + R_2 & -R_2 & 0 & \cdots & 0 \\ -R_2 & R_2 + R_3 & -R_3 & \cdots & 0 \\ 0 & -R_3 & R_3 + R_4 & \cdots & 0 \\ \vdots & \vdots & \vdots & \ddots & \vdots \\ 0 & 0 & 0 & \cdots & R_n \end{bmatrix}; \quad l_N = \begin{bmatrix} L_1 & 0 & 0 & \cdots & 0 \\ 0 & L_2 & 0 & \cdots & 0 \\ 0 & 0 & L_3 & \cdots & 0 \\ \vdots & \vdots & \vdots & \ddots & \vdots \\ 0 & 0 & 0 & \cdots & L_n \end{bmatrix};$$

$$23 m_N = \begin{bmatrix} (m_1 + m_2 + m_3 + \cdots + m_n) & 0 & 0 & \cdots & 0 \\ 0 & (m_2 + m_3 + \cdots + m_n) & 0 & \cdots & 0 \\ 0 & 0 & (m_3 + \cdots + m_n) & \cdots & 0 \\ \vdots & \vdots & \vdots & \ddots & \vdots \\ 0 & 0 & 0 & \cdots & m_n \end{bmatrix};$$

$$\ddot{\theta}_N = \begin{bmatrix} \ddot{\theta}_1 \\ \ddot{\theta}_2 \\ \ddot{\theta}_3 \\ \vdots \\ \ddot{\theta}_n \end{bmatrix}; \quad \dot{\theta}_N = \begin{bmatrix} \dot{\theta}_1 \\ \dot{\theta}_2 \\ \dot{\theta}_3 \\ \vdots \\ \dot{\theta}_n \end{bmatrix}; \quad \theta_N = \begin{bmatrix} \theta_1 \\ \theta_2 \\ \theta_3 \\ \vdots \\ \theta_n \end{bmatrix}; \quad \eta_{Na} = \begin{bmatrix} \dot{\eta} \\ \dot{\eta} \\ \dot{\eta} \\ \vdots \\ \dot{\eta} \end{bmatrix}$$

The case for 3-link, small-oscillations pendulum can be written as:

$$ML\ddot{\theta} + R\dot{\theta} + gml\theta + ml\eta_a = 0 \quad (\text{A-1})$$

where:

$$M = \begin{bmatrix} m_1L_1 & m_2L_1 & m_3L_1 \\ 0 & m_2L_2 & m_3L_2 \\ 0 & 0 & m_3L_3 \end{bmatrix}; \quad L = \begin{bmatrix} L_1 & 0 & 0 \\ L_1 & L_2 & 0 \\ L_1 & L_2 & L_3 \end{bmatrix}; \quad R = \begin{bmatrix} R_1 + R_2 & -R_2 & 0 \\ -R_2 & R_2 + R_3 & -R_3 \\ 0 & -R_3 & R_3 \end{bmatrix};$$

$$m = \begin{bmatrix} (m_1 + m_2 + m_3) & 0 & 0 \\ 0 & (m_2 + m_3) & 0 \\ 0 & 0 & m_3 \end{bmatrix}; \quad l = \begin{bmatrix} L_1 & 0 & 0 \\ 0 & L_2 & 0 \\ 0 & 0 & L_3 \end{bmatrix};$$

$$\ddot{\theta} = \begin{bmatrix} \ddot{\theta}_1 \\ \ddot{\theta}_2 \\ \ddot{\theta}_3 \end{bmatrix}; \quad \dot{\theta} = \begin{bmatrix} \dot{\theta}_1 \\ \dot{\theta}_2 \\ \dot{\theta}_3 \end{bmatrix}; \quad \theta = \begin{bmatrix} \theta_1 \\ \theta_2 \\ \theta_3 \end{bmatrix}; \quad \eta_a = \begin{bmatrix} \dot{\eta} \\ \dot{\eta} \\ \dot{\eta} \end{bmatrix};$$

This is in complete agreement with the well-known small oscillations model [21]. The first derivative separated version becomes

$$d\theta = L_E^{-1}M_E^{-1}(-G_E m_E l_E \theta_E - m_E l_E E) \quad (\text{A-2})$$

where $\theta_E = [u \ v \ w \ \theta_1 \ \theta_2 \ \theta_3]^T$; $E = [0 \ 0 \ 0 \ \dot{\eta} \ \dot{\eta} \ \dot{\eta}]^T$ are vectors and

$$M_E = \begin{bmatrix} M & R \\ 0 & I \end{bmatrix}; \quad L_E = \begin{bmatrix} L & 0 \\ 0 & I \end{bmatrix}; \quad m_E = \begin{bmatrix} 0 & m \\ I & 0 \end{bmatrix}; \quad l_E = \begin{bmatrix} I & 0 \\ 0 & L \end{bmatrix}$$

$$G_E = \begin{bmatrix} I & 0 \\ 0 & G \end{bmatrix}; G = \begin{bmatrix} g & 0 & 0 \\ 0 & g & 0 \\ 0 & 0 & g \end{bmatrix}$$

are 6x6 partitioned matrix:

1
2
3
4
5
6
7
8
9
10
11
12
13
14
15
16
17
18
19
20
21
22
23
24
25
26
27
28
29
30
31
32
33
34
35
36
37
38
39
40
41
42
43
44
45
46
47
48
49
50
51
52
53
54
55
56
57
58
59
60
61
62
63
64
65